Indian Journal of Pure & Applied Physics
Vol. 57, October 2019, pp. 773-782

Unsteady slip flow of amicropolarnanofluid over an impulsively stretched vertical surface

A M Rashad[a], Waqar A Khan[b], Iskander Tlili[c, d,]*& A M A EL-Hakiem[a]

[a]Department of Mathematics, Aswan University, Faculty of Science, Aswan 81528, Egypt

[b]Department of Mechanical Engineering, College of Engineering, Prince Mohammad Bin Fahd University, Al Khobar 31952, Kingdom of Saudi Arabia

[c] Department for Management of Science and Technology Development, Ton Duc Thang University, Ho Chi Minh City, Vietnam

[d] Faculty of Applied Sciences, Ton Duc Thang University, Ho Chi Minh City, Vietnam

Received 2 April 2018; accepted 4 January 2019

The unsteady mixed convective flow of micropolarnanofluid over an impulsively stretched vertical surface has been examined. A model has been developed to analyze the behavior of nanofluids in presentmicropolar fluids studied numerically for both cases of assisting and opposing flow taking into account the thermal convective boundary condition. A model has been developed to analyze the behavior of nanofluids containing metallic nanoparticles as copper (Cu)and nonmetallic nanoparticles as alumina (Al_2O_3) in water-micropolarnanofluidhave been considered. The governing partial differential equations have been transformed to non-similar differential equations then have been solved numerically by using theRunge-Kutta-Fehlberg method of seventh order (RKF7). The results have been compared with the published results and are found in excellent agreement.

Keywords: Micropolar fluid, Unsteady mixed convection, Nanofluid, Stretched vertical surface

1 Introduction

Conventional heat transfer fluids such as oil, water, and ethylene glycol play an important role in scientifically, industrial and engineering processes[1]. The heat transfer improvements are necessary in the development and manufacturing of electronic devices. Many researchers studied the stagnation flow and heat transfer problems for stretching surfaces with different forms of stretching velocity, one of them; Ramachandran *et al*.[2] studied the mixed convection in stagnation flows adjacent to vertical surface. The unsteady mixed convection in the stagnation flow on a heated vertical plate is studied by Seshadri *et al.*[3] Choi[4] introduced an innovative technique, which used a mixture of nanoparticles and the base fluid in order to develop advanced heat transfer fluids with substantially higher conductivities. He referred to the resulting mixture as a nanofluid. Jang and Choi[5] were the first to use the term 'nanofluid' to refer to a fluid in which nanoparticles are suspended. Nanofluid is considered one of the efficient passive strategies in heat transfer enhancement for the purpose of improving the efficiency of many thermal systems such as: solar collectors, thermal storage, cooling of (electronic components, transformers and engine/vehicle) and nuclear reactors. When nanofluids used in automobile cooling system (radiator), then the heat rejected will be large enough in such a way that the radiator is not necessary placed in the automobile front, this enables redesigning the automobile with less drag front which in turn reduces fuel consumption up to 5%.Nanofluid has high thermophysical properties in thermal conductivity and convective heat transfer coefficient and thus is expected to increase the heat transfer performance of the base fluids[6]. Many researchers in recent years have been interested in studying the nanofluid and many studies related to nanofluids characteristics are very well described in the book by Das *et al.*[7] and in the review papers by Buongiorno[8], Kakaç and Pramuanjaroenkij[9], Wang and Mujumdar[10]. Kuznetsov and Nield[11] studied the problem of natural convection boundary layer flow of a nanofluid past a vertical flat plate. Khan and Pop[12]have analyzed the problem of steady boundary layer flow, heat transfer and nanoparticle fraction over a stretching surface in a

*Corresponding author (E-mail: iskander.tlili@tdtu.edu.vn)

nanofluid. Syakila and Pop[13] studied steady mixed convection boundary layer flow past a vertical flat plate embedded in porous medium filled with nanofluids is studied using different types of nanoparticles. The problem of free convection boundary layer of non-Newtonian fluid along a vertical cone embedded in a porous medium saturated with nanofluid is considered by Rashad*et al*.[14]. They studied the problem of mixed convection flow of a nanofluid from a horizontal circular cylinder embedded in a porous medium with convective boundary condition. Chamkha*et al*.[15,16] studied the problems of mixed convection boundary layer flow over a wedge and cone embedded in a porous medium. Rashad *et al*.[17] presented the problem of natural convection boundary layer flow adjacent to a vertical cylinder embedded in a thermally satisfied nanofluid saturated non-Darcy porous medium. Rashad *et al*.[18] have analyzed the problem of mixed convection flow of a nanofluid from horizontal circular cylinder embedded in a porous medium with convective boundary condition. Hakiem and Rashad[19] have considered unsteady mixed convection flow of a nanofluid over an impulsively stretched vertical surface under convective boundary condition.

The micropolar fluid theory is a fluid flow theory which takes into consideration the micro rotation of a nanoparticles that could potentially clarify the theoretically and the experimental results. Physically, the micropolar fluids may characterize fluids consisting of rigid, randomly spherical (or oriented) particles suspended in a viscous medium, where the deformation of fluid particles is ignored. Eringen[20] introduced that the Navier-stokes equations can be considered as a micropolar fluid. Micropolar fluid is defined as a fluid with microstructure which belongs to a class of fluids with non-symmetric stress tensors. Eringen[21] also developed the theory of thermomicropolar fluids by extending the theory of micropolar fluids.Some applications of micropolar fluid mechanics have been given by Ariman *et al*.[22] They studied the inadequacy of the classical Navier-Stokes theory to describe rheological complex fluids such as liquids crystals, which has led to the development of micro continuum fluid mechanics as an extension of the classical theory.Aziz[23] presented an analysis for the unsteady mixed convection flow of a viscous incompressible micropolar fluid adjacent to a heated vertical surface in the presence of viscous dissipation when the buoyancy force assists or opposes the flow. Recently, there are useful books of micropolar theory by Lukaszewicz[24] and Eringen[25]. Takhar *et al*.[26] had carried out a research on mixed convection flow of a micropolar fluid over a stretching sheet. Nazar *et al*.[27]had studied similar problem but for the stagnation point case. Khan *et al*.[28] had solved alike problem for nanofluid. Ahmed and Rashad[29] investigated the effects of anisotropic porous medium on the natural convection of micropolarnanofluids inside a rectangular enclosure. Also, a thermal stratification and suction/injection effects on flow and heat transfer of micropolar fluid due to stretching cylinder is analyzed by Mansour *et al*.[30] Cheng[31]investigated the natural convection boundary layer flow of a micropolar fluid near a vertical permeable cone with variable wall temperature.

The principle goal of this work is to study unsteady mixed convection boundary layer and heat transfer of a nanofluid flow over a heated vertical linearly stretched sheet in a micropolar fluid with both of assisting and opposing external laminar flow taking in to account the thermal convective boundary condition.

2 Problem Formulations

Consider unsteady mixed convection boundary layer flow and heat transfer of micropolar nanofluids over a heated vertical linearly stretched surface for both cases of assisting and opposing flow with the impacts of the thermal convective boundary condition and partial slip. Two equal and opposite forces are impulsively applied along the x-axis so that the wall is stretched, keeping the origin fixed in the nanofluid of ambient temperature T_∞. It is maintained that the sheet surface is heated by convection from a hot fluid at the temperature T_f which provides a heat transfer coefficient h_f, is to be suddenly increased or decreased to the value T_∞. The sheet surface is either heated or cooled by convection from a ferrofluid of temperature T_f such that $T_f > T_\infty$ corresponding to a heated surface (assisting flow) and $T_f < T_\infty$ corresponding to a cooled surface (opposing flow), respectively. Initially $(t < 0)$, the sheet has uniform temperature T_∞ and it is at rest in an unbounded quiescent fluid having constant temperature T_∞. At t=0, the sheet surface is impulsively stretched with velocity $U_e(x)=ax$ which varies linearly with the distance x along the, and the temperature at the sheet surface is suddenly changed to constant values $T_f > T_\infty$ and subsequently maintained

at that temperature surface. The flow is assumed to be laminar and a micropolar nanofluid is given to be Newtonian, incompressible and electrically conducting with uniform properties and thermal equilibrium between the in a water-based micropolar nanofluid containing different type of nanoparticles: Copper (Cu), and nonmetallic nanoparticles, alumina (Al_2O_3). Thermophysical properties of the nanofluid are presented in Table 1(Sheikholeslami and Bandpy[24]). The thermophysical properties of water and nanoparticles are presented in Table 2 for the micropolar nanofluid are also assumed to be fixed except for the density variation in the buoyancy force, which is evaluated based on the Boussinesq approximation. Considering the famous formulation of Tiwari and Das[14], thus the fundamental equations under the Boussinesq approximation for unsteady flow are(Ishak *et al.*[25]):

$$\frac{\partial u}{\partial x}+\frac{\partial v}{\partial y}=0, \qquad \ldots(1)$$

$$\frac{\partial u}{\partial t}+u\frac{\partial u}{\partial x}+v\frac{\partial u}{\partial y}= \left(\frac{\mu_{nf}+\kappa}{\rho_{nf}}\right)\frac{\partial^2 u}{\partial y^2}+\frac{\kappa}{\rho_{nf}}\frac{\partial N}{\partial y}+\frac{g^*(\rho\beta)_{nf}}{\rho_{nf}}(T-T_\infty), \quad \ldots(2)$$

$$\rho_{nf}\, j\left(\frac{\partial N}{\partial t}+u\frac{\partial N}{\partial x}+v\frac{\partial N}{\partial y}\right)=\gamma_{nf}\frac{\partial^2 N}{\partial y^2}-\kappa\left(2N+\frac{\partial u}{\partial y}\right), \quad \ldots(3)$$

$$\frac{\partial T}{\partial t}+u\frac{\partial T}{\partial x}+v\frac{\partial T}{\partial y}=\alpha_{nf}\frac{\partial^2 T}{\partial y^2}. \qquad \ldots(4)$$

The corresponding initial and boundary conditions for this problem can be written as:

$$t<0: u=v=0, T=T_\infty \text{ at any } x, y$$

$$t\geq 0: u=U_e+N_1\mu_{nf}\frac{\partial u}{\partial y}, v=0, N=$$

$$-n\frac{\partial u}{\partial y}, -k_{nf}\frac{\partial T}{\partial y}=h_f\left(T_f-T\right) \text{ at } y=0$$

$$u\to 0, T\to T_\infty \text{ at } y\to\infty, \qquad \ldots(5)$$

where t, x and y represent time, tangential distance, and transverse or normal distance, respectively. u, v and T are the fluid tangential velocity, normal velocity and the nanofluid temperature, respectively. g^* and h_f are the acceleration due to gravity and heat transfer coefficient, respectively. a is constant and $U_e=ax$, is the velocity of the wall at $t>0$. ρ_{nf} is the is the effective density of the nanofluid, μ_{ff} is the effective dynamic viscosity of the nanofluid and α_{nf} is

Table 2 – Thermo-physical properties of water and nanoparticles [37].

Property	Pure water	Copper (Cu)	Alumina Al_2O_3
ρ(kg m^{-3})	997.1	8933	3970
C_p (Jkg^{-1} K^{-1})	4179	385	765
k (W m^{-1} K^{-1})	0.613	401	40
β (K^{-1})	21 × 10^{-5}	1.67 × 10^{-5}	0.85 × 10^{-5}

Table 1 – Comparison of $f''(\xi,0)$ and $-\theta'(\xi,0)$ for different values of λ and Pr for (ϕ=κ= 0 and $Bi\to\infty$) at ξ=1.0 (steady-state flow).

Pr	λ	Ishak *et al.*[31]		Present results	
		$f''(1,0)$	$-\theta'(1,0)$	$f''(1,0)$	$-\theta'(1,0)$
0.7	0	-1.0000	0.7937	-1.00000	0.79371
	1.0	-0.5076	0.8961	-0.50763	0.89613
	10	2.5777	1.1724	2.57772	1.17244
	100	21.8052	1.8075	21.80527	1.80756
1.0	0	-1.0000	1.0000	-1.00000	1.00000
	1.0	-0.5608	1.0873	-0.56081	1.08733
	10	2.3041	1.3716	2.30414	1.37164
	100	20.3786	2.0667	20.37862	2.06673
3.0	0	-1.0000	1.9237	-1.00000	1.92374
	1.0	-0.7092	1.9743	-0.70924	1.97433
	10	1.4567	2.2442	1.45673	2.24424
	100	15.9716	3.1042	15.97168	3.10427
7.0	0.0	-1.0000	3.0722	-1.00000	3.07221
	1.0	-0.7962	3.1055	-0.79621	3.10553
	10	0.8505	3.3318	0.85054	3.33185
	100	12.7216	4.2663	12.72167	4.26636

the thermal diffusivity of the nanofluid, $(\rho C_p)_{nf}$ is the heat capacitance of nanofluid, $(\rho\beta)_{nf}$ is the thermal expansion coefficient of the nanofluid which are given by (Tiwari and Das[14]):

$$\rho_{nf}=(1-\phi)\rho_f+\phi\rho_S,\ \mu_{nf}=\frac{\mu_f}{(1-\phi)^{2.5}},\ \alpha_{nf}=\frac{k_{nf}}{(\rho C_p)_{nf}},\ (\rho\beta)_{nf}=(1-\phi)(\rho\beta)_f+\phi(\rho\beta)_S,$$

$$\gamma_{nf}=\left(\mu_{nf}+\kappa/2\right)j=\mu_f\left(\mu_{nf}+K/2\right)j$$

$$\gamma_{nf}=\left(\mu_{nf}+\kappa/2\right)j=\mu_f\left(\mu_{nf}/\mu_f+K/2\right)j,$$

$$(\rho C_p)_{nf}=(1-\phi)(\rho C_p)_f+\phi(\rho C_p)_s. \qquad \ldots(6)$$

Here, ϕ is the is the nanoparticle volume fraction parameter, μ_f is the dynamic viscosity of the basic fluid, β_f and β_s are the thermal expansion coefficients of the base fluid and nanoparticle, respectively, ρ_f and ρ_s are the densities of the basic fluid and nanoparticle, respectively, k_{nf} is the effective thermal conductivity of nanofluid which is given as:

$$\frac{k_{nf}}{k_f}=\frac{(k_s+2k_f)-2\phi(k_f-k_s)}{(k_s+2k_f)+\phi(k_f-k_s)}, \qquad \ldots(7)$$

where, k_s is the thermal conductivity of the nanoparticles and k_f is the thermal conductivity of base fluid.

It is convenient to non-dimensionalize and transform Eq. (1) through Eq. (4) by using:

$$\psi=(a\upsilon_f)^{1/2}\xi^{1/2}xf(\xi,\eta),N=ax(a/\upsilon_f)^{1/2}\xi^{-1/2}g(\xi,\eta),\ \eta=(a/\upsilon_f)^{1/2}\xi^{-1/2}y,\xi=1-e^{-t^*},$$

$$t^*=at,\theta(\xi,\eta)=\frac{T-T_\infty}{T_f-T_\infty},u=\frac{\partial\psi}{\partial y},v=-\frac{\partial\psi}{\partial x}. \qquad \ldots(8)$$

Substituting Eqs. (5-8) into Eq. (1) through Eq. (4) leads the following non-dimensional equations:

$$(\Gamma_1+\Gamma_4)f'''+\Gamma_4 g'+\frac{1}{2}\eta(1-\xi)f''+\xi\left(ff''-f'^2+\lambda\Gamma_2\theta\right)=\xi(1-\xi)\frac{\partial f'}{\partial\xi}, \qquad \ldots(9)$$

$$(\Gamma_1+\Gamma_4/2)g''+\frac{1}{2}(1-\xi)(\eta g'+g)+\xi(fg'-f'g)-\xi\Gamma_4 B(2g+f'')=\xi(1-\xi)\frac{\partial g}{\partial\xi}, \qquad \ldots(10)$$

$$\frac{\Gamma_3}{\Pr}\frac{k_{nf}}{k_f}\theta''+\frac{1}{2}\eta(1-\xi)\theta'+\xi f\theta'-\xi f'\theta=\xi(1-\xi)\frac{\partial\theta}{\partial\xi}, \qquad \ldots(11)$$

where, Eq. (1) is identically satisfied. In Eqs. (9-11), the prime indicates differentiation with respect to η and the parameters Γ_1, Γ_2 and Γ_3 are given by:

$$\Gamma_1(\phi)=\frac{1}{(1-\phi)^{2.5}\left[1-\phi+\phi\left(\rho_S/\rho_f\right)\right]},$$

$$\Gamma_2(\phi)=\frac{\left[1-\phi+\phi\left((\rho\beta)_S/(\rho\beta)_f\right)\right]}{\left[1-\phi+\phi\left(\rho_S/\rho_f\right)\right]},$$

$$\Gamma_4(\phi)=\frac{K}{\left[1-\phi+\phi\left(\rho_S/\rho_f\right)\right]},K=\frac{\kappa}{\mu_f},B=\frac{\upsilon_f}{aj},$$

$$\Gamma_3(\phi)=\frac{1}{\left[1-\phi+\phi\left((\rho C_p)_S/(\rho C_p)_f\right)\right]}. \qquad \ldots(12)$$

The transformed initial and boundary conditions become:

$$f(\xi,0)=0,f'(\xi,0)=1+\frac{\delta\xi^{-1/2}}{(1-\phi)^{2.5}}f''(\xi,0),g(\xi,0)=-nf''(\xi,0),\frac{k_{nf}}{k_f}\theta'(\xi,0)=-Bi\xi^{1/2}\left[1-\theta(\xi,0)\right]$$

$$f'(\xi,\infty)=0,\theta(\xi,\infty)=0, \qquad \ldots(13)$$

Here $\lambda=Gr_x/\mathrm{Re}_x^2$ is the mixed convection parameter, $Gr_x=g^*\beta_f\left(T_f-T_\infty\right)x^3/\upsilon_f^2$ is the local Grashof number, $\mathrm{Re}_x=\left(U_e x/\upsilon_f\right)$ is the local Reynolds numbers, $Bi=h_f\left(\upsilon_f/a\right)^{1/2}/k_f$ is the Biot number, $\delta=N_1\mu_f(a/\upsilon_f)^{1/2}$ is the slip factor, $\Pr=\upsilon_f(\rho C_p)_f/k_f$ is the Prandtl number. It should be noted that $\lambda>0$ is for heated surface (assisting flow),

λ<0 is for cooled surface (opposing flow) and λ=0 corresponds to the forced convection flow. Further, ϕ =0 corresponds to a regular fluid and $Bi\rightarrow\infty$ to the isothermal surface. In this case, Eqs (9-11) reduce to those for the problem of unsteady mixed convection boundary-layer flow over an impulsively stretched vertical surface reported by Ishak *et al.*[25] as $\phi=\kappa=0$ and $Bi\rightarrow\infty$.

Of special significance for this type of flow and heat transfer situation are the local skin-friction coefficient and local Nusselt number. These physical parameters can be defined in dimensionless form as:

$$C_{fx}=-\frac{\left(\mu_{nf}+\kappa\right)\left(\partial u/\partial y\right)_{y=0}+\left(\kappa N\right)_{y=0}}{\rho_f U_e^2}=$$

$$-\mathrm{Re}_x^{-1/2}\,\xi^{-1/2}\left(\frac{\mu_{nf}}{\mu_f}+K(1-n)\right)f''(\xi,0), \qquad \ldots(14)$$

$$Nu_x=-\frac{x\left(\partial T/\partial y\right)_{y=0}}{(T_f-T_\infty)}=-\mathrm{Re}_x^{-1/2}\,\xi^{-1/2}\left(\frac{k_{nf}}{k_f}\right)\theta'(\xi,0)\,. \qquad \ldots(15)$$

3 Numerical Method

The problem of unsteady mixed convective flow of micropolar nanofluid is investigated and a model is developed to analyze the behavior of nanofluids numerically for both cases of assisting and opposing flow taking into account the thermal convective boundary condition. The governing partial differential equations are converted into non-linear ordinary differential equations by using suitable transformations. These equations are solved numerically by means of Runge-Kutta-Fehlberg method of seventh order (RKF7).The details of this method can be finding in literature[38]. The convergence is assumed to be 10^{-6}.

4 Results and Discussion

An unsteady mixed convective flow of micropolar nanofluid over an impulsively heated stretched vertical surface in the presence of metallic and nonmetallic nanoparticles taking in account thermal convective boundary condition and partial slip has been investigated.

The effect of solid volume of nonmetallic nanoparticles Al_2O_3 on dimensionless velocity for both heated and cooled surface are depicted in Fig. 1(a and b), respectively, with other parameters maintained constant slip factor δ=0.1 and Biot number Bi=10.As expected, the dimensionless velocity is maximum for dimensionless boundary layer thickness η=0 correspond to y=0 which means near the vertical surface then tend to zero while moving away of vertical linearly stretched surface. It can be seen that that the velocity profile increases significantly with respect to assisting flows while it decrease meaningfully with opposing flows, therefore, the thickness of hydrodynamic boundary layer also depends upon. It indicates that applying assisting flows effect which means that the surface is heated (λ > 0), leads to a thermal buoyancy forces manifested by a substantial overshoot in the dimensionless velocity near the vertical stretched surface for higher λ nonetheless for lower heated surface $0.1\leq\lambda\leq 10$ the overshoot in velocity profile disappear. It should be noted that for opposing flow (λ<0) which means that the surface is cooled therefore the thermal buoyancy forces lessens the dimensionless velocity expressively within the boundary layer and opposite flows arises for λ=-50 at η=1. It is further observed that the

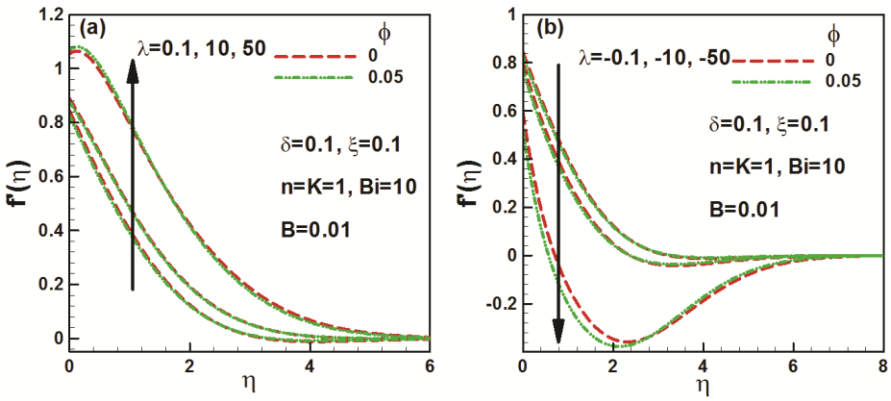

Fig. 1 – Effect of solid volume of Al_2O_3 nanoparticles on dimensionless velocity for early initial unsteady (a) assisting and (b) opposing flows.

volume fraction of Al_2O_3 has neglected effect on dimensionless velocity; this can be attributed to the lesser density of Al_2O_3 nanoparticles.

The effects of solid volume of metallic nanoparticles Cu on dimensionless velocity for both assisting and opposing flows are illustrated in Figs 2(a) and 1(b), respectively, with other parameters maintained constant slip factor δ=0.1 and Biot number B_i=10. It is remarked that the dimensionless velocity increase with mixed convection parameter λ in case of applying assisting flows however, it decreases when applying opposing flows (λ<0). It is found that the dimensionless velocity has the similar behavior for both Al_2O_3 and Cu nanoparticles, nevertheless we realize that the magnitude of the overshoot in velocity profile near the vertical surface increases with metallic than nonmetallic nanoparticles. This is due to the fact that the influence of thermal buoyancy force is more pronounced in case of metallic nanoparticles due to the higher density of the copper (Cu) compared to alumina (Al_2O_3), therefore, the dimensionless velocity augment in the boundary layer as the assisting flows simulate gradient pressure. It is worthwhile to note that Fig. 2 proves that the volume fraction of Cu nanoparticles affects clearly the velocity profile more than Al_2O_3 nanoparticles, It indicates that the dimensionless velocity decreases with solid volume of Cu nanoparticle, this can be interpreted by the fact that the Al_2O_3 nanoparticles has less density than Cu nanoparticles.

Figure 3(a, b) displays the variation of dimensionless temperature with solid volume of Al_2O_3 nanoparticles and mixed convection parameter λ for both assisting and opposing flows with further parameters reserved constant, respectively. It can be seen that the temperature profile has moderate increasing with volume fraction of Al_2O_3, whereas it decline with mixed convection parameter in case of assisting flow λ>0 and increase for opposing flows λ<0, therefore the thickness of thermal boundary layer also depends upon. In an unexpected and perplexing results, it is therefore found that the assisting/opposing flows parameters have no effects on the thermal boundary layer thickness, this can be elucidated by the fact that assisting/opposing flows parameters affect meaningfully the velocity profile which leads to no

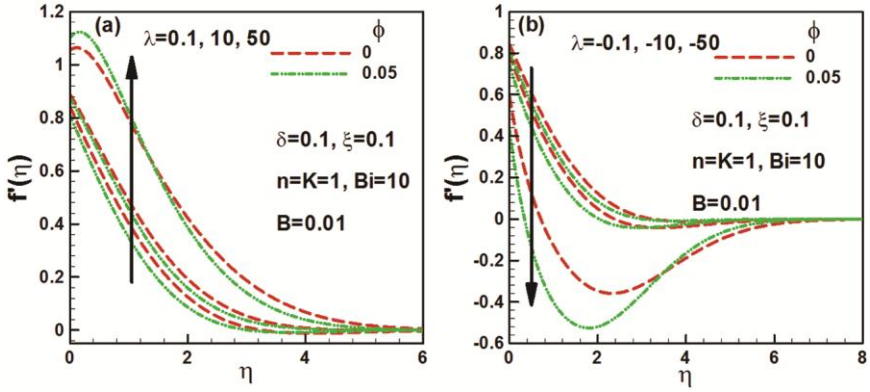

Fig. 2 – Effect of solid volume of Cu nanoparticles on dimensionless velocity for early initial unsteady (a) assisting and (b) opposing flows.

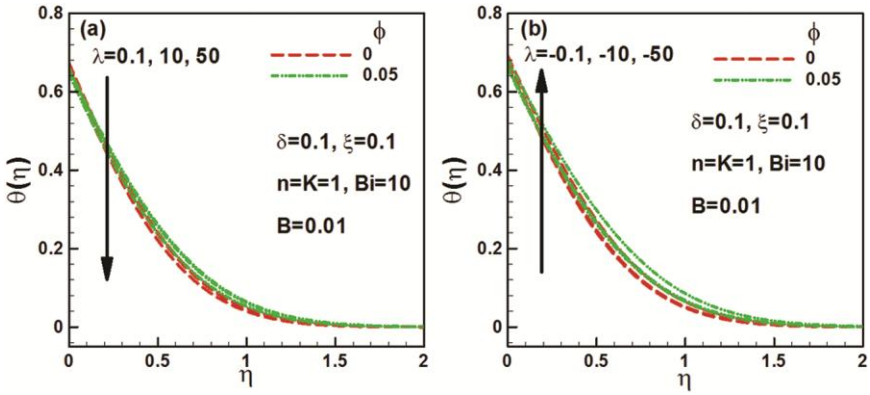

Fig. 3 – Effect of solid volume of Al_2O_3nanoparticles on dimensionless temperature for early initial unsteady (a) assisting and (b) opposing flows.

enough time for unsteady mixed convective flow to get heat from the stretched vertical surface. Moreover, the effect of λ is more pronounced in velocity profile than temperature profiles for the reason that λ not involved precisely in Eq. (11). It is meaningful to note that for the case of regular fluid (ϕ=0) the assisting and opposing flows does not affect the temperature profile.

Figure 4(a, b) exhibits, respectively, the variation of dimensionless temperature with solid volume of Cu nanoparticles and mixed convection parameter λ for both assisting and opposing flows, other parameters are kept constant. It is found that the dimensionless temperature has the similar behavior for both Al_2O_3 and Cu nanoparticles, as observed that the dimensionless temperature declines with η from highest value for η=0 to zero value for η=2. It can be interpreted from Figs 3 and 4 that changing nanoparticles form nonmetallic nanoparticles Al_2O_3 to metallic nanoparticles Cu does not alters temperature profile which means that in this case nanoparticle density does not affect dimensionless temperature, therefore the thickness of thermal boundary layer remains unvarying regarding density of nanoparticles.

The effect of solid volume of nonmetallic nanoparticles Al_2O_3 on skin friction in fully developed flow regime for assisting and opposing flows are presented respectively in Fig. 5 (a, b). It is perceived that the skin friction decreases expressively along the stretched vertical surface, this behavior is in good agreement with the Eq. (12), moreover the skin friction lessen with both volume fraction and mixed convection parameter λ in case of assisting flow, while it increases with mixed convection parameter λ in case of opposing flow. It can be interpreted on this fact that the increasing on velocity profile which in turn leads to augment Reynolds number and as exposed in Eq. (12) that the skin friction decrease with Reynold number, moreover augmenting on Reynolds number leads to reduce viscous forces compared to inertial forces which in turn shearing stress declines, subsequently, the skin friction decreases. It is important to note that the effect of opposing flows on skin friction in fully developed flow regime is more pronounced that of assisting flow, the physical reason behind this is that the pressure near the stretched vertical surface is greater than far from the surface due to manifested thermal buoyancy forces.

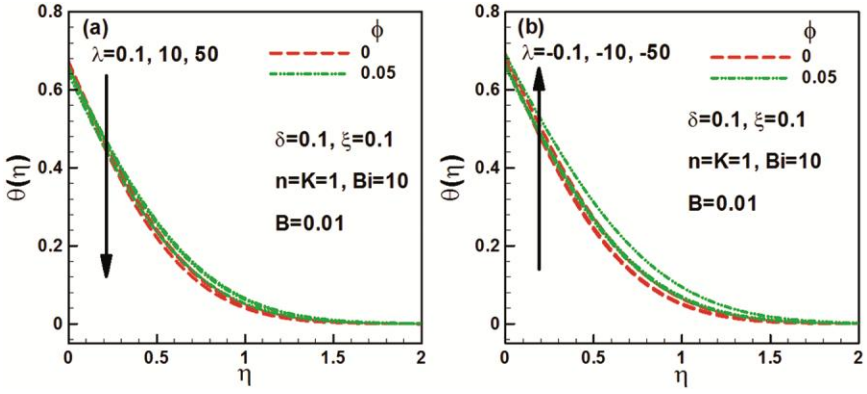

Fig. 4 – Effect of solid volume of Cu nanoparticles on dimensionless temperature for early initial unsteady (a) assisting and (b) opposing flows.

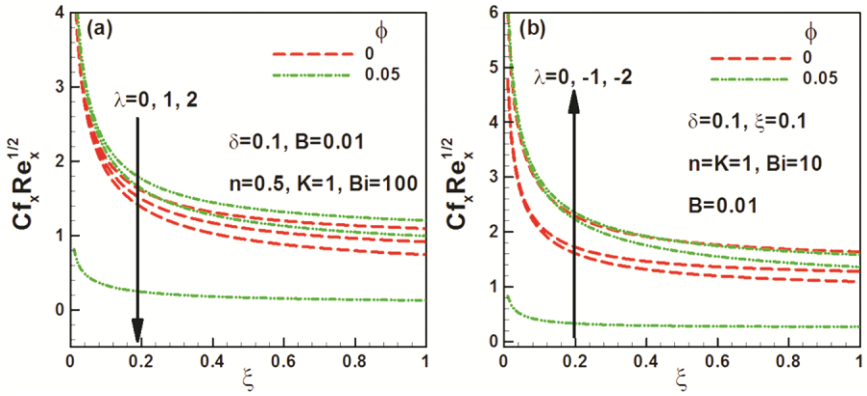

Fig. 5 – Effect of solid volume of Al_2O_3 nanoparticles on skin friction in fully developed flow regime for (a) assisting and (b) opposing flows.

Figure 6 (a, b) present, respectively, the effect of solid volume of Cu nanoparticles on skin friction in fully developed flow regime for assisting and opposing flows, other parameters are kept constant. The skin friction for the metallic nanoparticle Cu declines sensitively along the stretched vertical surface as in case on nonmetallic nanoparticles Al_2O_3. It is found that the solid volume fraction and mixed convection parameter λ for both case assisting and opposing flows have the same effect on skin friction for metallic nanoparticle Cu and for nonmetallic nanoparticles Al_2O_3. It is further observed that for both nanoparticles Al_2O_3 and Cu, the skin friction has the highest value at the commencing of stretched vertical surface and drops up to zero at ξ=1. This is due to growth in the dimensionless velocity inside the boundary layer with respect to mixed convection parameter as revealed by Figs 1 and 2 and consequently leads to intensification in the boundary layer thickness. It is worthwhile to note that for highest value of both solid volume fraction and mixed convection parameter the skin friction is very small for mutually metallic and nonmetallic nanoparticles.

The effect of solid volume of Al_2O_3 nanoparticles on dimensionless heat transfer rate in fully developed flow regime for assisting and opposing flows are exposed, respectively, in Fig. 7 (a and b), with other parameters sustained constant slip factor δ=0.1 and Biot number B_i=100.As observed the heat transfer rate decreases with along the stretched vertical surface attaining the highest value at the beginning of stretched vertical surface and drops up to minimal value at ξ=1. This effect is mathematically obvious in Eq. (13) showing Nusselt number.Additionally, the heat transfer rate increases with both solid volume ϕof Al_2O_3 nanoparticles and mixed convection parameter λ in case of assisting flows, whereas, it decreases with mixed convection parameter λ in case of opposing flows. Physically, this can be attributed to the increase of temperature gradient with respect to solid volume fraction as revealed by Fig. 3 (a, b). It is valuable to note that the heat transfer rate for regular fluid (water ϕ=0) are lesser and augment with volume fraction of nanoparticle, this can be interpreted by the fact that increasing on solid volume fraction of nanoparticles leads to augment the thermal

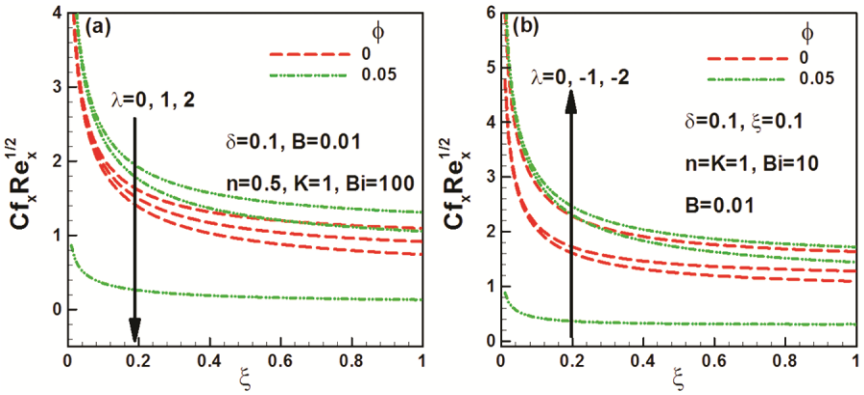

Fig. 6 – Effect of solid volume of Cu nanoparticles on skin friction in fully developed flow regimefor (a) assisting and (b) opposing flows.

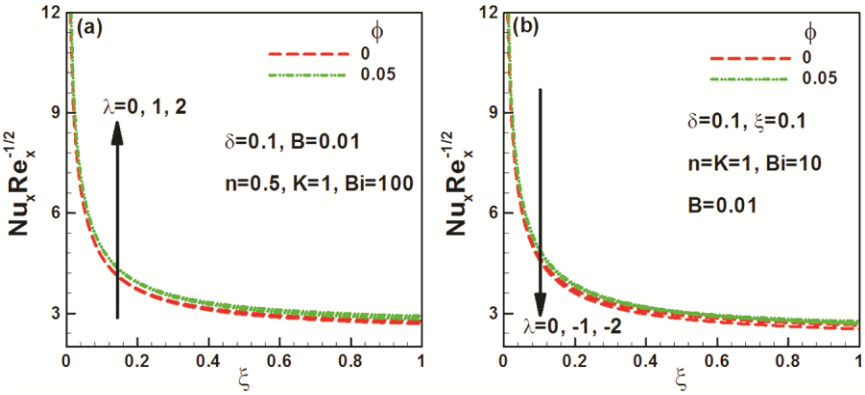

Fig. 7 – Effect of solid volume of Al_2O_3 nanoparticles on dimensionless heat transfer rate in fully developed flow regimefor (a) assisting and (b) opposing flows.

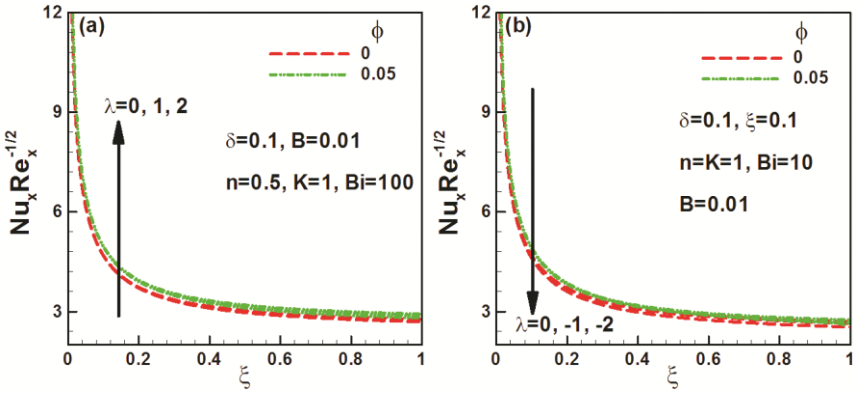

Fig. 8 – Effect of solid volume of Cu nanoparticles on dimensionless heat transfer rate in fully developed flow regimefor (a) assisting and (b) opposing flows.

conductivity. Nevertheless, the effects of mixed convection parameter on the heat transfer rate are not noticeable.

Figure 8 (a, b) depict, respectively, the effect of solid volume of Cu nanoparticles on dimensionless heat transfer rate in fully developed flow regime for assisting and opposing flows, with other parameters kept fixed: slip factor δ=0.1 and Biot number B_i=100. As shown in Fig. 7 in case of metallic nanoparticle Cu, the heat transfer rate dropalong the stretched vertical surface from the highest value at the beginning of stretched vertical surface and lessen to minimal value at ξ=1. We realize that the heat transfer rate behaviors for both metallic and nonmetallic nanoparticle are similar. It can be interpreted on this fact that the convective heat transfer is dominant compared to conductive heat transfer one at the beginning of stretched vertical surface and along the surface the conductivity will be dominant.

5 Conclusions

An unsteady mixed convective flow of nanofluids containing metallic nanoparticles (Cu) and nonmetallic nanoparticles (Al_2O_3) in water-micropolar nanofluid for both cases of assisting and opposing flow over an impulsively heated stretched vertical surface in the presence of partial slip thermal convective boundary condition and has been inspected numerically by means of Runge-Kutta-Fehlberg method of seventh order (RKF7).

The comparative results presented for the case of metallic and non-metallic nanoparticles for both assisting and opposing flows are mentioned as follows:

(i) The velocity profile increases significantly with respect to assisting flows while it decreases meaningfully with opposing flows for both metallic and nonmetallic nanoparticle.

(ii) Metallic nanoparticle Cu alters significantly the dimensionless velocity more than nonmetallic nanoparticle Al_2O_3.

(iii) The temperature profile decreases with mixed convection parameter in case of assisting flow ($\lambda > 0$) and increases for opposing flows ($\lambda < 0$).

(iv) Changing nanoparticle from metallic (Cu) to nonmetallic (Al_2O_3)does not affect the thermal boundary layer thickness.

(v) The skin friction decreases expressively along the stretched vertical surface for both metallic and nonmetallic nanoparticle. Moreover, it decreases with both volume fraction and mixed convection parameter λ in case of assisting flow, while it increases with mixed convection parameter λ in case of opposing flow.

(vi) The effect of opposing flows (λ<0) on skin friction in fully developed flow regime is more pronounced that assisting flow (λ>0).

(vii) The heat transfer rate for regular fluid (ϕ=0) is lesser and augment with volume fraction of nanoparticle, nevertheless, the effects of mixed convection parameter on the heat transfer rate are not really noticeable.

References

1 Daungthongsuk W &Wongwises S, *Renew Sust Energy Rev*, 11 (2007) 797.

2 Ramachandran N, Chen T S & Armaly B F, *J Heat Transfer*, 3 (1988) 110.

3 Seshadri R, Sreeshylan N & Nath G,*Int J Heat Mass Transfer*, 45 (2002) 1345.

4 Choi S U S, *ASME Fluids Eng Div*, 231 (1995) 99.

5 Jang S P & Choi S U S, *ApplPhys*, 84 (2004) 4316.
6 Murshed S M S, Castro C A N D, Loureno M J V, Lopes M L M &Santo F J V, *Renew Sust Energ Rev*, 15 (2011) 2342.
7 Das S K, Choi S U S, Yu W & Pradeep T, *Nanofluids*, Science and Technology, (Wiley: New Jersey), (2007)*416*.
8 Buongiorno J, *ASME J Heat Transfer*, *128*(2006) 240.
9 KakacS & Pramuanjaroenkij A, *Int J Heat Mass Transfer*, 52 (2009) 3187.
10 Wang L & Fan J, *ASME J Heat Transfer*, 133 (2011) 040801.
11 Kuznetsov A V & Nield D A, *Int J Therm Sci*, 49 (2010) 243.
12 Khan WA & Pop I, *Int J Heat Mass Transfer*, 53 (2010) 2477.
13 Ahmed S & Pop I, *Int Commun Heat Mass Transfer*, 37 (2010) 987.
14 Chamkha AJ, Rashad AM & Abdou MMM, *Int J Microscale Nanoscale Therm Fluid Transp Phenom*, 2 (2011) 323.
15 Chamkha A J, Abbasbandy S, Rashad A M &Vajravelu K, *Transp Porous Med*, 91 (2012) 261.
16 Chamkha A J, Abbasbandy S, Rashad A M & Vajravelu K, *Meccanica*, 48 (2013) 275.
17 Rashad A M, AbbasbandyS & ChamkhaA J, *J Taiwan Inst Chem Eng*, 45 (2014) 163.
18 Rashad A M, Chamkha A J & Modather M, *Comput Fluids*, 86 (2013) 380.
19 El-Hakiem M A & Rashad A M, *J Comput Theor Nanosci*, 12 (2015) 1.
20 Eringen A C, *Int J EngSci*, 2 (1964) 205.
21 Eringen A C, *J Math Anal Appl*,38 (1972) 480.
22 Ariman T, Turk MA & Sylvester ND, *Int J Eng Sci*, 11 (1973) 905.
23 El-Aziz A M, *J Egypt Math Soc*, 21 (2013) 385.
24 Lukaszewicz G, *Micropolar Fluids, Theory and Applications*, (Basel:Birkhuser), (1999).
25 Eringen AC, *Microcontinuum Field Theories*, II Fluent Media, (Springer: New York), (2001).
26 Takhar H S, Agarwal R S, Bhargava R & Jain S, *Int J Heat Mass Transfer*, 34 (1998) 213.
27 Nazar R, Amin N, Filip D & Pop I, *Int J Non-Linear Mech*, 39 (2004) 1227.
28 Khan WA & Pop I, *Int J Heat Mass Transfer*, 53 (2010) 2477.
29 Ahmed S E & Rashad A M, *J Porous Med*, 19 (2016) 737.
30 Tiwari RK & Das MK, *Int J Heat Mass Transfer*, 50 (2007) 2002.
31 Ishak A, Nazar R & Pop I, *Arab J Sci Eng*, 31 (2006) 165.
32 Rees D A S & Bassom A P, *Int J Eng Sci*, 34 (1996) 113.
33 Tlili I, *Symmetry*, 11(2019) 438.
34 GoodarziM, TliliI, Tian Z&Safaei M, *Int J Numer Methods Heat Fluid Flow*, (2019). https://doi.org/10.1108/HFF-12-2018-0730.
35 Afridi M I, Tlili I, Goodarzi M, Osman M & Khan N A, *Symmetry*, 11 (2019) 663.
36 Tlili I & Alkanhal T A, *J Water Reuse Desalination*, 24 (2019). https://doi.org/10.2166/wrd.2019.057.
37 I Tlili, Khan W A & Ramadan K, *J Nanofluids*, 8 (2019) 179.
38 Tlili I, Khan WA & Ramadan K, *J Nanofluids*, 7 (2018) 879.
39 Tlili I, Khan WA & Khan I, *Results Phys*, 8 (2018) 213.
40 Tlili I, Hamadneh NN & Khan W A, *Arab J Sci Eng*,(2018) 1.
41 Tlili I, Hamadneh N N, Khan W A & Atawneh S, *J Therm Anal Calorimetr*, 132 (2018) 1899.
42 Khan W A, Rashad A M, Abdou M MM & I Tlili, *Eur J Mech Fluids*, 75 (2019) 133.
43 Ahmadi G, *Int J Eng Sci*, 14 (1976) 639.
44 Jena S K & Mathur MN, *Int J Eng Sci*, 19 (1981) 1431.
45 Peddieson J, *Int J Eng Sci*, 10 (1972) 23.
46 Nazar R, Tham L, Pop I & Ingham D B, *Transp Porous Med*, 86 (2011) 517.
47 Oztop H F & Abu-Nada E, *Int J Heat Mass Transfer*, 29 (2008) 1326.
48 Mathews J H & Fink KK, *Numerical Methods Using Matlab*, 4thEdn, (Prentice-Hall Inc Upper Saddle River: New Jersey, USA), 2004.